

## Response for Editor

We greatly appreciate the Editor for very helpful comments. All comments were incorporated into the revised manuscript. The responses to individual comments are listed below.

**1) Please explicitly note the years in the caption of figures that show a comparison between models and observations.**

→ Thank you for your kind comment. We added the years in the caption of Fig. 1, 2, 3, 9, S1, S5, S6, and S7.

**2) Page 7 (line 239): I don't think this statement is accurate because RH doesn't have a linear relationship with moisture and temperature. Please revise or remove.**

→ We agree with your comment. We deleted the discussion regarding RH and modified the sentence as "More poleward transport of moisture in SAM0 enhances the NCD for cloud liquid." in line 238-239 in the revised manuscript.

**3) Page 7 (line 263): change "those with tops" to "fractional coverage of cloud"**

→ Thanks. We corrected it in line 262 in the revised manuscript.

**4) Page 8 (line 289): Please clarify "two radiations". Longwave and shortwave radiative fluxes?**

→ Following the comment, we clarified the sentence by saying that with "the net forcing of SW and LW radiation" in line 291 in the revised manuscript.

**5) Page 8 (line 295-297): I don't think this statement of causal relationship is supported here. The smaller snow depth and surface albedo can be due to other factors such as less snowfall, not necessarily the warmer temperature. Please revise.**

→ Thank you very much for the comment. We agree with your comment. To address your comment, we corrected the sentence as "It is possible that the associated increase of  $T_{2m}$  from CAM5 to SAM0 in the Arctic pole decreases snow depth, but other factors (e.g., less snowfall) may also be responsible for this decrease." in line 297-299 in the revised manuscript.

**6) Page 8 (line 299): change "charges" to "changes"**

→ Thanks. We corrected it in line 300 in the revised manuscript.

**7) Page 9 (line 327-330): This can be removed or needs to be elaborated.**

→ Thanks. We deleted the paragraph in the revised manuscript.

Additionally, we got the professional English editing service, which corrected some wordings and grammar, but did not change the context of the draft.

# Impact of poleward heat and moisture transports on Arctic clouds and climate simulation

Eun-Hyuk Baek<sup>1</sup>, Joo-Hong Kim<sup>2</sup>, Sungsu Park<sup>3\*</sup>, Baek-Min Kim<sup>4\*</sup>, Jee-Hoon Jeong<sup>1</sup>

<sup>1</sup>Faculty of Earth System and Environmental Sciences, Chonnam National University, 77 Yongbong-ro, Buk-gu Gwangju, 61186, South Korea

<sup>2</sup>Unit of Arctic Sea-Ice Prediction, Korea Polar Research Institute, 26 Songdomirae-ro, Yeosu-gu, Incheon, 21990, South Korea

<sup>3</sup>School of Earth and Environmental Sciences, Seoul National University, 1 Gwanak-ro, Gwanak-gu, Seoul, 08826, South Korea

<sup>4</sup>Department of Environmental Atmospheric Sciences, Pukyong National University, 49 Yongso-ro, Nam-gu, Busan, 48513, South Korea

Correspondence to: Sungsu Park (sungsup@snu.ac.kr) and Baek-Min Kim (baekmin@pknu.ac.kr)

**Abstract.** Many **general circulation models** (GCMs) have difficulty **simulating** Arctic clouds and climate, causing **substantial** inter-model spread. To address this issue, two Atmospheric Model Inter-comparison Project (AMIP) simulations from the Community Atmosphere Model version 5 (CAM5) and Seoul National University (SNU) Atmosphere Model version 0 (SAM0) with a Unified Convection Scheme (UNICON) are employed to identify **an effective** mechanism **for** improving Arctic **cloud** and climate **simulations**. Over the Arctic, SAM0 **produced a larger** cloud fraction and cloud liquid mass than CAM5, reducing the negative Arctic **cloud** biases in CAM5. The analysis of cloud water condensate rates indicates that this improvement is associated with an enhanced net condensation rate of water vapor into the liquid condensate of Arctic low-level clouds, which in turn is driven by enhanced poleward transports of heat and moisture by **the** mean meridional circulation and transient eddies. The reduced Arctic cloud biases lead to improved simulations of surface radiation fluxes and near-surface air temperature over the Arctic throughout the year. The association between the enhanced poleward transports of heat and moisture and **increase in** liquid clouds over the Arctic is also evident not only in both models, but also in the multi-model analysis. Our study **demonstrates** that enhanced poleward heat and moisture transport in a model can improve simulations of Arctic clouds and climate.

## 1 Introduction

With **the** increasing **amounts of** greenhouse gases, the Arctic has undergone the most rapid warming **of any location** on Earth. During the last decade, the warming rate of the near-surface air temperature over the Arctic has been two to three times that of the entire globe (Johannessen et al., 2016; Screen and Simmonds, 2010; Serreze and Barry, 2011). This pronounced Arctic temperature amplification, some of which is forced by the positive feedbacks among various climate components (e.g., sea ice albedo feedback (Deser et al., 2000), water vapor and cloud feedback (Lu and Cai, 2009), **and** lapse-rate feedback (Pithan et al., 2014)), is also responsible for extreme weather and climate events over mid-latitude continents (Kug et al., 2015; Screen and Simmonds, 2013; Wu and Smith, 2016). Most **general circulation models** (GCMs) struggle to **simulate the Arctic climate properly, producing results with** excessive cold surface temperature. The inter-GCM spread of greenhouse-induced warming is the largest over the Arctic (Boe et al., 2009; de Boer et al., 2012; Chapman and Walsh, 2007; Karlsson and Svensson,

Deleted: General Circulation Models

Deleted: in

Deleted: a large

Deleted: from the

Deleted: the

Deleted: that works on

Deleted: clouds

Deleted: simulation

Deleted: simulates more

Deleted: clouds

Deleted: the

Deleted: more

Deleted: demonstrated

Deleted: as well as

Deleted: General Circulation Models

Deleted: properly

Deleted: , suffering from the

2013). Many ~~researchers have~~ reported that the GCM-simulated cold biases over the Arctic are associated with the ~~shortwave (SW) and longwave (LW) radiation biases~~ at the surface, which are due to poor simulation of Arctic clouds (Barton et al., 2014; English et al., 2015; Karlsson and Svensson, 2013; Shupe and Intrieri, 2004). Over the Arctic, many GCMs underestimate the cloud fraction (de Boer et al., 2012; Cesana and Chepfer, 2012; English et al., 2015; Kay et al., 2016) and cloud liquid mass (Cesana et al., 2015; English et al., 2014; Kay et al., 2016). Because ~~liquid-containing clouds (i.e., mixed-phase clouds) have larger optical depths~~ than pure ice clouds (King et al., 2004; Shupe and Intrieri, 2004), ~~reduced~~ cloud liquid mass causes weaker cloud radiative forcing in GCMs. Unlike ~~at midlatitudes, mixed-phase clouds over the Arctic can persist for several days~~ (Morrison et al., 2011; Shupe et al., 2011). From a process perspective, cloud liquid in ~~mixed-phase clouds~~ should be rapidly depleted into cloud ice within a few hours owing to the higher saturation vapor pressure over water compared with ~~that over ice (i.e., the Wegener–Bergeron–Findeisen (WBF) mechanism) (Bergeron, 1935; Findeisen, 1938; Wegener, 1911).~~ Therefore, to sustain cloud liquids for several days, a certain production mechanism ~~is necessary~~ to counteract the WBF depletion process. Morrison et al. (2011) reviewed various candidate production processes for cloud liquid in Arctic mixed-phase clouds, such as the compensating feedback between the formation and growth of cloud liquid droplets and ice crystals (Jiang et al., 2000; Prenni et al., 2007), in-cloud turbulence generated by cloud top radiative cooling (Korolev and Field, 2008; Shupe et al., 2008), and horizontal advection by large-scale flows (Sedlar and Tjernström, 2009; Solomon et al., 2011). More ~~recently, researchers have~~ also noted that ice nucleation may be important for correctly simulating Arctic mixed-phase clouds. Liu et al. (2011) demonstrated that their revised ice nucleation scheme increased ~~the~~ cloud liquid mass in ~~Arctic mixed-phase stratocumulus clouds and the~~ associated downward LW flux at the surface during the Fall 2004 Mixed-Phase Arctic Cloud Experiment (MPACE). Subsequent sensitivity studies with various ice nucleation schemes ~~yielded~~ similar results (English et al., 2014; Xie et al., 2013). These improvements are attributed to the revised ice nucleation that decelerates the WBF depletion process in ~~mixed-phase clouds~~. Even with ~~increased~~ cloud liquid mass, ~~the~~ low-level cloud fraction ~~decreased in the~~ simulations, such that the ~~radiation flux biases~~ at the surface and ~~top of the atmosphere (TOA) still remained.~~

~~To~~ determine the factors responsible for the negative biases in GCM-simulated cloud liquid mass and cloud fraction over the Arctic, ~~in this study,~~ the Arctic climate simulated by the Seoul National University Atmosphere Model version 0 with a Unified Convection Scheme (SAM0-UNICON; Park, 2014a, 2014b; Park et al., 2017; Park et al., 2019) ~~is compared~~ to that of the Community Atmosphere Model version 5 (CAM5; Neale et al., 2012; Park et al., 2014). By comparing ~~the~~ two Atmospheric Model Intercomparison Project (AMIP) simulations, CAM5 and SAM0-UNICON, we ~~elucidate~~ 1) the ~~differences~~ in ~~the~~ cloud properties over the Arctic as simulated by SAM0-UNICON and CAM5, 2) the mechanisms of ~~cloud simulation improvement~~, and 3) the ~~effects of cloud~~ simulation on the Arctic climate simulation. ~~Section 2 describes the model design and data used in this study.~~ Section 3.1 ~~presents the results of the Arctic cloud simulations and related mechanisms, and Section 3.2 describes the effects of Arctic clouds on the Arctic climate simulations.~~ Finally, Section 4 ~~provides a summary and discussion.~~

Deleted: studies

Deleted: biases of

Deleted: radiations

Deleted: the

Deleted: a

Deleted: depth

Deleted: less

Deleted: in

Deleted: the

Deleted: the

Deleted: needs

Deleted: recent studies

Deleted: the

Deleted: reported

Deleted: the

Deleted: the

Deleted: increase,

Deleted: still

Deleted: biases of the

Deleted: fluxes

Deleted: the

Deleted: -

Deleted: -

Deleted: In an attempt to

Deleted: ,

Deleted: will compare

Deleted: with

Deleted: will show

Deleted: difference

Deleted: the improved clouds

Deleted: influence

Deleted: clouds

Deleted: Model

Deleted: will be described in

Deleted: 2. The

Deleted: clouds simulation

Deleted: mechanism will be provided in

Deleted: 1. The impact

Deleted: simulation will be presented in Section 3.2.

Deleted: will be provided in Section 4

## 2 Method

### 2.1 Model and experimental design

SAM0-UNICON (Park et al., 2019), hereinafter, referred to as SAM0, for simplicity, is an international GCM participating in the Coupled Model Intercomparison Project 6 (CMIP6) (Eyring et al., 2016). SAM0 is based on CAM5, but adopts the Unified Convection Scheme (UNICON) (Park, 2014a, 2014b) instead of the shallow (Park and Bretherton, 2009) and deep convection schemes (Zhang and McFarlane, 1995) of CAM5; further, it has a revised treatment of the cloud macrophysics process (Park et al., 2017). Other features, such as the dynamic core, cloud macrophysics and microphysics schemes, planetary boundary layer (PBL) scheme, etc. are exactly the same in both models. UNICON is a process-based subgrid convection parameterization scheme consisting of multiple convective updrafts, convective downdrafts, and subgrid cold pools and mesoscale organized flow without relying on any equilibrium constraints, such as convective available potential energy (CAPE) or convective inhibition (CIN) closures. UNICON simulates all dry-moist, forced-free, and shallow-deep convection within a single framework in a seamless, consistent, and unified manner (Park, 2014a, 2014b). The revised cloud macrophysics scheme diagnoses additional detrained cumulus by assuming a steady-state balance between the detrainment rate of cumulus condensates and the dissipation rate of detrained condensates by entrainment mixing (Park et al., 2017). The addition of detrained cumulus substantially improves the simulation of low-level clouds and the associated cloud radiative forcing in the subtropical trade cumulus regime. Park et al. (2019) showed that the global mean climate, 20th century global warming, and El Niño and Southern Oscillation, simulated by SAM0 are roughly similar to those of CAM5 and the Community Earth System Model version 1 (CESM1; Hurrell et al., 2013); however, SAM0 substantially improves the simulations of Madden-Julian Oscillation (MJO) (Madden and Julian, 1971), the diurnal cycle of precipitation, and tropical cyclones, all of which are known to be extremely difficult to simulate in GCMs.

To evaluate the impact of SAM0 on the Arctic cloud system, we conducted five ensemble experiments of an AMIP simulation for 36 years from January 1979 to February 2015 with a horizontal resolution of 1.9° latitude × 2.5° longitude and with 30 vertical layers for both CAM5 and SAM0. The climatology from the two simulations over the Arctic is then compared. The detailed settings of the AMIP simulations is identical to those described in Park et al. (2014). For rational comparison with satellite observation data, the model cloud fraction is calculated using the lidar simulator in the Cloud Feedbacks Model Intercomparison Project (CFMIP) Observation Simulator Package (COSP) diagnostic model. A detailed description of the COSP diagnostic model can be found in Kay et al. (2012).

### 2.2 Observational data

The observed Arctic cloud fraction and condensate phase information are obtained from the Cloud-Aerosol Lidar and Infrared Pathfinder Satellite Observations (CALIPSO)–GCM Oriented CALIPSO Cloud Product (CALIPSO–GOCCP) from June 2006 to November 2010 (Chepfer et al., 2010). The lidar beam of CALIPSO may not detect a few ice crystals underneath optically thick stratocumulus clouds due to attenuation and CALIPSO–GOCCP may slightly underestimate the ice clouds in the lowest levels at midlatitudes and in polar regions (Cesana et al., 2015). Nevertheless, CALIPSO–GOCCP currently provides the best available satellite observations of polar clouds because it can detect optically thin clouds without relying on the albedo or thermal contrast (Cesana and Chepfer, 2012; Kay et al., 2012). The observed TOA fluxes are obtained from version 2.8 of the Clouds and Earth's Radiant

Deleted: ,

Deleted: ,

Deleted: , however

Deleted:

Deleted: , and

Formatted: Font: 10 pt

Deleted: for

Deleted: -

Deleted: -

Deleted: -

Deleted:

Deleted: (ENSO)

Deleted: the

Deleted: x

Deleted: are

Deleted: are

Deleted: a

Deleted: the

Deleted: its

Deleted: the

Deleted: the

190 Energy System (Wielicki et al., 1996) Energy Balanced and Filled data (Loeb et al., 2009) (CERES–EBAF) from  
 March 2000 to February 2013. Although CERES–EBAF ~~likely~~ exceeds the global uncertainty particularly for  
 clear sky ~~retrieval over the Arctic~~ due to the low albedo contrast between snow and clouds, it is the only available  
 source of basin-wide TOA fluxes in the Arctic, and newer versions have advanced to distinguish clouds from  
 underlying high-albedo sea ice and snow cover by utilizing cloud radiances from the collocated Moderate  
 195 Resolution Imaging Spectroradiometer (MODIS) and sea ice concentration fields from the National Snow and Ice  
 Data Center (NSIDC) (English et al., 2014). The climatology data of long-term ground-based cloud and radiation  
 measurements from 1998 to 2010 at the North Slope of Alaska (NSA) Barrow site (71~~°~~ ~~38°~~ N, 156~~°~~ ~~68°~~ W) from  
 the Atmospheric Radiation Measurement (ARM) Best Estimate (ARMBE) dataset (Xie et al., 2010) are used for  
 the model evaluation. The Arctic near-surface air temperature at a ~~height of 2 m~~ ( $T_{2m}$ ), liquid water path (LWP),  
 200 and ice water path (IWP) are obtained from the European Center for Medium-Range Weather Forecasts (ECMWF)  
 ERA-Interim reanalysis dataset from January 1979 to February 2015 (Dee et al., 2011).

### 2.3 CMIP5 models

To identify the relationship between the Arctic clouds and poleward transports of moisture and heat, we also  
 analyzed AMIP simulations of ~~Coupled Model Intercomparison Project Phase 5~~ (CMIP5) (Taylor et al., 2012).  
 205 We used the outputs from nine models (bcc-csm1-1-m, CanAM4, CNRM-CM5, GFDL-CM3, HadGEM2-A,  
 IPSL-CM5A-MR, IPSL-CM5B-LR, MIROC5, and MPI-ESM-LR), which can be accessed from  
<http://pcmdi.llnl.gov/>. These models are selected based on the availability of the following model outputs: monthly  
 low-cloud fraction calculated ~~using the~~ CALIPSO COSP diagnostic model (variable name: clcalipso), liquid  
 water path (variable name: clwvi), ice water path (variable name: clivi), daily meridional wind (variable name:  
 210 va), air temperature (variable name: ta), and specific humidity (variable name: hus).

## 3 Results

### 3.1 Arctic clouds and their relationships with poleward moisture and heat transports

SAM0 reduces the negative biases of CAM5 in cloud fraction and liquid cloud simulations. Figure 1a shows the  
 annual cycle of the total cloud fraction (TCA) averaged over the Arctic area (north of 65° N) obtained from  
 215 CAM5, SAM0, and observation. Consistent with Kay et al. (2012) and English et al. (2014), CAM5  
 underestimates the observed TCA throughout the year. The negative biases in the CAM5-simulated TCA are  
 reduced in SAM0, which simulates a more realistic TCA, particularly during summer. SAM0 improves not only  
 the cloud fraction but also the simulation of cloud phase characteristics. Cesana et al. (2015) proposed the height  
 at which the ratio of cloud ice mass to total cloud condensate mass is 90 % (i.e., the phase ratio, PR90) as a useful  
 220 indicator in assessing the model performance to simulate the cloud phase. ~~For~~ most GCMs, ~~PR90~~ is ~~lower~~ than  
~~the~~ satellite observation ~~height~~, implying that most GCMs underestimate cloud liquid mass or overestimate cloud  
 ice mass. Both CAM5 and SAM0 underestimate ~~the~~ cloud liquid mass over the Arctic; however, SAM0 ~~yields~~  
 better estimates ~~than~~ CAM5 (Fig. 1b). Not only the biases against satellite observation, ~~but also~~ the biases against  
 ground-based observation are ~~reduced~~ in SAM0. Figure 2 shows the annual ~~cycles~~ of TCA, LWP, surface  
 225 downward ~~SW~~ radiation (FSDS), and surface downward ~~LW~~ radiation (FLDS) from CAM5, SAM0, and the  
 observation at ~~the~~ Barrow site. TCA is less ~~in the CAM5 results than in~~ the observation except ~~in~~ July and August.

Deleted: over the Arctic

Deleted: retrievals

Deleted: 38N

Deleted: 68W

Deleted: 2 m

Deleted: the

Deleted: by

Deleted: The obtained PR90 in

Deleted: located at heights

Deleted: that of

Deleted: exhibits

Deleted: compared with

Deleted: also

Formatted: Font: Times New Roman

Deleted: cycle

Deleted: short-wave

Deleted: long wave

Deleted: barrow

Deleted: in CAM5

Deleted: that of

Deleted: for

LWP is also underestimated over the entire period. Accordingly, the downward ~~SW~~ flux is overestimated and the downward ~~LW~~ flux is underestimated, particularly in autumn and winter. Although TCA in SAM0 is overestimated in ~~summer~~ compared with the observation, SAM0 reduces the bias of CAM5 during the other periods. The ~~simulated LWP is~~ closer to the observation than ~~that obtained using~~ CAM5. Biases of the surface radiation fluxes are also reduced, except during ~~summer~~.

Figure 3 shows the annual-mean vertical profiles of ~~the~~ grid-mean cloud condensate masses and the ~~cloud fraction differences~~ between SAM0 and CAM5 averaged over the Arctic area. Compared with CAM5, SAM0 simulates more cloud liquid condensate mass in the lower troposphere but slightly less cloud ice condensate mass throughout the troposphere (~~Figs. 3b and 3c~~). Thus, the total cloud condensate mass ~~increases (decreases)~~ in the lower troposphere (~~mid-troposphere~~) from CAM5 to SAM0, respectively, which is responsible for the difference in the cloud fraction (~~Figs. 3a and 3d~~). The increase in the cloud liquid condensate mass reduces ~~the~~ bias against the ERA-interim reanalysis. CAM5 underestimates both ~~the~~ cloud liquid and ice condensation against ~~that in~~ the reanalysis (~~Supplements S1b and S1e~~). SAM0, however, simulates cloud liquid condensation close to ~~that in~~ the reanalysis, although the cloud ice condensation is underestimated as much as ~~that obtained using~~ CAM5 (~~Supplements S1c and S1f~~). These changes ~~in~~ cloud characteristics from CAM5 to SAM0 differ from ~~those in~~ previous ~~reports~~ on the ~~effects~~ of revised ice nucleation ~~schemes~~ (English et al., 2014; Liu et al., 2011; Morrison et al., 2008), ~~in~~ which a smaller (larger) low-level (mid-level) cloud fraction ~~was simulated~~. The increase (decrease) of cloud liquid (ice) mass is consistent with the increase ~~in~~ PR90 ~~height~~ from CAM5 to SAM0, as shown in Fig. 1b.

To understand the physical processes responsible for the increases ~~in the~~ cloud fraction and cloud liquid mass in the lower troposphere from CAM5 to SAM0, we plotted the annual-mean vertical profiles of the grid-mean tendencies of cloud liquid and ice condensate masses averaged over the Arctic ~~from various physical processes~~ (Fig. 4). Both CAM5 and SAM0 ~~show~~ two main physical processes generating Arctic cloud liquid condensate: the net condensation of water vapor into cloud liquid (NCD) simulated by the cloud macrophysics scheme and the convective detrainment of cloud liquid (DET). In contrast, two main depletion processes are ~~the~~ precipitation–sedimentation fallout of cloud condensate (PRS) and WBF conversion of cloud liquid into cloud ice (WBF) simulated by the cloud microphysics scheme. For cloud ice condensate, the main sources are the net deposition of water vapor into cloud ice (NCD), WBF, and convective detrainment of cloud ice (DET), while the main sink is PRS (Fig. 4b). With the exception within the ~~PBL~~, below 950 hPa, the grid-mean tendencies due to subgrid vertical transports of cloud condensates by local symmetric turbulent eddies (PBL) and nonlocal asymmetric turbulent eddies (CON) are generally smaller than ~~the~~ other tendencies. Near the surface, the PBL scheme operates as a strong source for cloud liquid owing to downward vertical transport of cloud liquid mass from the cloud layers above (Fig. 4a).

The largest ~~differences~~ between CAM5 and SAM0 ~~are~~ in NCD and DET, particularly for cloud liquid. For cloud liquid, SAM0 simulates ~~a~~ weaker DET but much stronger NCD than CAM5, such that the sum of NCD and DET simulated by SAM0 is larger than that of CAM5, with ~~a~~ maximum difference of approximately  $0.05 \text{ g kg}^{-1} \text{ day}^{-1}$  around 850 hPa, where the differences ~~in the~~ cloud liquid condensate mass and cloud fraction between CAM5 and SAM0 are also ~~maximized~~ (see Fig. 3b). ~~These findings indicate~~ that the increases ~~in the~~ cloud fraction and cloud liquid condensate mass from CAM5 to SAM0 are mainly ~~due to~~ an enhanced NCD for cloud liquid from CAM5 to SAM0. The differences in PBL and CON between CAM5 and SAM0 are relatively small. For cloud ice, the

Deleted: shortwave

Deleted: longwave

Deleted: summertime

Deleted: LWP is

Deleted: those in

Deleted: summertime

Deleted: difference of

Deleted: Fig

Deleted: in the

Deleted: Fig

Deleted: its

Deleted: Supplementary

Deleted: the

Deleted: Supplementary

Deleted: of

Deleted: report

Deleted: impact

Deleted: scheme

Deleted: simulated

Deleted: .

Deleted: of

Deleted: heights

Deleted: of

Deleted: area

Deleted: shows

Deleted: observed:

Deleted: Planetary Boundary Layer (

Deleted: )

Deleted: difference

Deleted: is observed

Deleted: the

Deleted: the

Deleted: of

Deleted: maximum

Deleted: This indicates

Deleted: of

Deleted: caused by

overall production rate simulated by SAM0 is smaller than that of CAM5, mainly due to the decreases in NCD and DET slightly compensated by the increases in WBF and PRS, which leads to the decrease ~~in~~ cloud ice mass, as shown in Fig. 3c. The SAM0-simulated WBF tendency is slightly larger than that of CAM5 partly due to the larger cloud liquid mass in SAM0. In summary, the increases ~~in~~ cloud liquid mass, cloud fraction, and PR90 from CAM5 to SAM0 shown in Figs. 1 and 3 (which are improvements) are mainly ~~due to~~ the enhanced NCD for cloud liquid from CAM5 to SAM0. In accordance with the stronger NCD for liquid, the liquid cloud fraction ~~is~~ also ~~increased~~ to satisfy the saturation equilibrium constraint for cloud liquid (see Appendix A of Park et al. (2014)). ~~However, the~~ question ~~regarding~~ what physical process ~~caused~~ the increase ~~in~~ NCD for cloud liquid from CAM5 to SAM0 remained. In ~~both~~ models, the NCD for cloud liquid is explicitly calculated by the saturation equilibrium in the cloud microphysics scheme, which indicates that ~~a greater~~ NCD for cloud liquid is produced with more water vapor and lower temperature (Park et al., 2014). Assuming that the Arctic region is a cylinder, the water vapor over the Arctic region can be increased only ~~in~~ two ways: convergence of meridional moisture flux and surface moisture flux. Because the difference ~~in~~ surface moisture flux between the two models is much smaller than ~~the difference in~~ the convergence of meridional moisture flux ~~in the~~ Arctic region (compare ~~Supplement S2a~~ with S2b), ~~it can be~~ inferred that the difference in the large-scale horizontal advection of moisture from sub-Arctic to Arctic ~~causes~~ the increase in the Arctic water vapor source. Figure 5 shows the differences ~~in the~~ zonal-mean meridional transports of heat and moisture ~~in the~~ high-latitude region and vertical profiles of water vapor (Q), air temperature (T), and relative humidity (RH) averaged over the Arctic area. The zonal-mean meridional flux ~~can be~~ calculated as ~~shown in~~ Eq. (1):

$$[\overline{vX}] = [\overline{v}][\overline{X}] + [\overline{v'X'}] + [\overline{v''X''}], \quad (1)$$

where  $X = Q$  or  $T$ ;  $v$  is the meridional velocity; the ~~overbars~~ and ~~primes~~ denote time-mean and departure from the time-mean, respectively; and the square ~~brackets~~ and ~~asterisks~~ denote zonal-mean and departure from the zonal-mean, respectively. The first term on the right-hand side is the flux ~~due to~~ the mean meridional circulation, the second term is the flux ~~caused by~~ stationary ~~eddies~~, and the last term is the flux ~~due to~~ transient ~~eddies~~.

In the midlatitude and subpolar regions, SAM0 simulates poleward transports of heat and moisture more than CAM5, particularly in the lower troposphere (Figs. 5a and 5e), mainly due to enhanced transports by mean meridional circulation and transient eddies (Figs. 5b, ~~5c~~, ~~5f~~, and ~~5g~~). The difference ~~in~~ poleward moisture (heat) transport between SAM0 and CAM5 is approximately 10% (15%) of ~~the~~ climatology, respectively. The enhanced poleward transports of heat and moisture in SAM0 reduces its ~~bias~~ against the ERA-Interim reanalysis compared with CAM5. CAM5 overestimates both ~~the~~ moisture and heat fluxes over the midlatitude region against the reanalysis but underestimates those on the periphery (around ~~70°~~ N) of the Arctic circle (~~Supplement S3~~). Although the positive bias over the midlatitude region ~~remains~~, SAM0 reduces the biases of CAM5 on the periphery (around ~~70°~~ N) of the Arctic circle (~~Supplement S4~~). In the northern hemisphere, SAM0 simulates higher pressure and temperature in the low-latitude region but lower pressure and temperature in the high-latitude region compared with CAM5, which reduces the bias of CAM5 (~~Supplement S5~~). The circulation change in SAM0 enhances the mean meridional circulation and polar jet stream over higher latitudes (Li and Wang, 2003). The associated strengthening of ~~the~~ zonal mean meridional wind in the midlatitude region (see the contour lines in Figs. 5b and 5f) enhances the poleward transports of heat and moisture near the surface. ~~The enhanced~~ polar jet stream (see the contour lines in Figs. 5c and 5g) strengthens the storm track activity on the periphery of the Arctic circle (between 60° N and 70° N) (~~Supplements S5c and S5f~~) and increases the associated poleward transports of

Deleted: of

Deleted: of

Deleted: caused by

Deleted: increases

Deleted: The

Deleted: on

Deleted: has

Deleted: of

Deleted: the

Deleted: more

Deleted: by

Deleted: of

Deleted: that of

Deleted: Supplementary

Deleted: we

Deleted: caused

Deleted: of

Deleted: is

Deleted: :

Deleted: overbar

Deleted: prime

Deleted: bracket

Deleted: asterisk

Deleted: by

Deleted: eddy

Deleted: by

Deleted: eddy

Deleted: -c

Deleted: 5f-g

Deleted: of

Deleted: biases

Deleted: 70°

Deleted: Supplementary

Deleted: still

Deleted: 70°

Deleted: Supplementary

Deleted: Supplementary

Deleted: Enhanced

Deleted: Supplementary



heat and moisture by transient eddies. Moreover, SAM0 simulates the convection more strongly than CAM5, particularly in most of the tropical ocean, which reduces the bias from the reanalysis (Supplement S6). Several previous studies have shown that enhanced convective activity in the tropics enhances the poleward heat and moisture transport by inducing Rossby wave trains from the tropics toward the pole promoting warm and moist advection from midlatitudes to the Arctic (Lee et al., 2014; Fluorny et al., 2015). As with those studies, SAM0 seems to capture Rossby wave trains emanating from the tropics better than CAM5 (Supplement S5c), leading to enhanced poleward heat and moisture transport in SAM0.

Consequently, SAM0 simulates higher  $Q$ ,  $T$ , and  $RH$  than CAM5 over the Arctic (Figs. 5d and 5h). More poleward transport of moisture in SAM0 enhances the NCD for cloud liquid, as shown in Figs. 3b and 4a. Because the liquid cloud fraction is a function of the grid-mean  $RH$  in both models, the cloud fraction increases in the lower troposphere (i.e., below 700 hPa), as shown in Fig. 3d. In addition, warming associated with enhanced poleward heat transport and condensation heating is likely to reduce the amount of cloud ice mass from CAM5 to SAM0, as shown in Fig. 3c, hence reducing the ice cloud fraction in the mid-troposphere (i.e., above 700 hPa) formulated as a function of cloud ice condensate mass in both models (Fig. 2d).

The relationships between the poleward moisture transport and NCD for cloud liquid are well reflected by the seasonal and interannual variabilities in both models (Figs. 6 and 7). SAM0 simulates more poleward moisture transport into the Arctic than CAM5 throughout the year (Fig. 6). In both models, the poleward moisture transports at  $65^\circ N$  is the largest from summer to autumn, and the associated NCD for cloud liquid averaged over the Arctic region nearly agrees with the poleward moisture transport. The seasonal variability of the NCD difference for cloud liquid is almost coincident with that of  $RH$ , which explains the increase in the Arctic liquid cloud fraction from May to September, as shown in Fig. 1. The interannual variations of the poleward moisture transport and NCD for cloud liquid in each model are also highly correlated with the correlation coefficients of 0.84 and 0.81 for CAM5 and SAM0, respectively (Figs. 7a and 7b). In addition, in almost all years, SAM0 simulates more poleward moisture flux and higher NCD for cloud liquid over the Arctic than CAM5, and the inter-model differences of these variables are also highly correlated (Fig. 7c). In summary, the strengthened poleward moisture transport increases NCD for cloud liquid, cloud liquid mass, and cloud fraction from CAM5 to SAM0.

The close association between the Arctic cloudiness and poleward transports of heat and moisture, as demonstrated by the analysis of the CAM5 and SAM0 simulation results, also exist in other climate models. Figure 8 shows the scatter plots between the annual mean meridional transports of heat and moisture at  $65^\circ N$  and Arctic cloudiness and the LWP ratio (i.e., the ratio of LWP to the total condensate water path,  $LWP/(LWP+IWP)$ ) obtained from the analysis of various AMIP simulations of CMIP5 models. Wide inter-model spread exists in the TCA, low cloud fraction (LCA, defined as fractional coverage by clouds between the surface and 700 hPa), LWP ratio, and poleward transports of heat and moisture. Except for a few outliers (e.g., bcc-csm1-1-m and MPI-ESM-LR), there is a clear inter-model proportional relationship between the meridional moisture transport and TCA and LCA (Figs. 8a and 8b). All of the models simulate consistently positive poleward moisture transport. However, some models simulate equatorward heat transport at  $65^\circ N$ , and the corresponding LWP ratio over the Arctic tends to be smaller than those from the models with poleward heat transport (Fig. 8c). The models with strong poleward moisture transport tend to have strong poleward heat transport as well. The inter-model analysis supports our conclusion that poleward moisture and heat transport is one of the key factors controlling the LCA and LWP in the Arctic.

Deleted: Supplementary

Deleted: Tropics

Deleted: Tropics

Deleted: midlatitude into

Deleted: Tropics

Deleted: Supplementary

Deleted: )

Deleted: simulated

Deleted: T

Deleted: Notably, although SAM0 has a higher temperature than CAM5 in the Arctic,  $RH$  in SAM0 is higher than CAM5, which reveals that the increase in

Deleted: moisture

Deleted: into the Arctic is relatively larger than the increase in temperature. This indicates that the poleward moisture transport into the Arctic is one

Deleted: dominant factors for

Deleted: generation of

Deleted: .

Deleted: ;

Deleted: ,

Deleted: .

Deleted: shown in

Deleted:  $65^\circ$

Deleted: are

Deleted: agree

Deleted: (Figs. 7a and 7b),

Deleted: .

Deleted: shown from

Deleted: simulations

Deleted: those with tops

Deleted: Fig



### 3.2 Impact of Arctic clouds on the Arctic climate

Clouds play a critical role in the surface radiative balance as a climate regulator in the Arctic region. Figure 9 shows the biases of LCA, the upward LW radiation flux at the TOA (FLUT), and  $T_{2m}$  during winter obtained from CAM5 and SAM0. As shown, CAM5 suffers from negative biases of LCA, FLUT, and  $T_{2m}$  during December, January, and February (DJF) (Fig. 9, left panel). In the Arctic during winter, the lower LCA in CAM5 reduces FLUT over the land and sea-ice region in the lower troposphere because the temperature in the cloudy layer is higher than that at the surface (i.e., temperature inversion). The lower LCA also reduces the downward LW radiation at the surface (FLDS), which leads to colder near-surface air than in the reanalysis and thus enhances the temperature inversion. Compared with CAM5, SAM0 simulates greater LCA, FLUT, and  $T_{2m}$  over the entire Arctic (Fig. 9, center panel), such that their negative biases in CAM5 are alleviated by SAM0 (Fig. 9, right panel). Over the ocean where temperature inversion does not exist, the greater LCA in SAM0 results in more FLUT than in CAM5 (Fig. 9e). SAM0 also simulates stronger FLDS than CAM5 over the entire Arctic, as expected (not shown).

Not only the biases during DJF, but also the summer biases of TCA, SW cloud radiative forcing at the TOA (SWCF), and  $T_{2m}$  are also reduced from CAM5 to SAM0 (Fig. 10). In most Arctic areas except for some portions of the northern continents, CAM5 yielded negative TCA bias during June, July, and August (JJA) (Fig. 10a). SAM0 simulated a greater TCA than CAM5 (Fig. 10b), such that most of the negative TCA biases in CAM5 over the Arctic sea ice and open ocean areas disappear (Fig. 10c). The increase of TCA in SAM0 causes the SWCF to decrease (Fig. 10e), which also reduces positive SWCF bias in the vicinity of the Arctic pole (Fig. 10f). In the Arctic during summer, cloudiness has the opposite effect on SWCF and LWCF (Supplement S7); thus, it is necessary to examine the net forcing of SW and LW radiation at the surface to determine the impact of Arctic clouds on the Arctic climate. With greater TCA than CAM5, SAM0 simulates more net LW radiation at the surface (FLNS, Fig. 11b). Owing to the high albedo of the underlying sea ice and snow in the vicinity of the Arctic pole, the net SW radiation at the surface (FSNS) does not change much there; however, FSNS decreases substantially in the regions surrounding the Arctic pole (Fig. 11a). Overall, the increase in FLNS dominates over the decrease in FSNS at the Arctic pole, while the opposite is true in the surrounding regions (Figs. 11b and 11c). The net forcing of SW and LW radiation at the surface causes  $T_{2m}$  to increase at the Arctic pole and decrease in the surrounding continental area from CAM5 to SAM0 (Fig. 10h). It is possible that the associated increase of  $T_{2m}$  from CAM5 to SAM0 in the Arctic pole (Fig. 10h) decreases snow depth, but other factors (e.g., less snowfall) may also be responsible for this decrease (Fig. 11d). Less snow depth results in lower surface albedo (Fig. 11e). The enhanced SWCF cooling near the Arctic pole in SAM0 (Fig. 10e) is the combined results of the increased TCA and decreased surface albedo. If the Arctic sea ice fraction is allowed to change in response to the changes in the overlying atmospheric conditions (e.g., coupled simulation), SAM0 is likely to simulate a lower sea ice fraction than CAM5 due to the increased TCA and warmer near-surface air temperature, which can be further accelerated by the positive surface albedo feedback (Holland and Bitz, 2003). In fact, Park et al. (2019) found that SAM0 simulates lower sea ice fraction than CESM1 (coupled model of CAM5; Hurrell et al., 2013) over the Arctic in a 20th century coupled simulation.

**Deleted:** top of the atmosphere (...OA)... (FLUT), and  $T_{2m}$  during wintertime...inter obtained from CAM5 and SAM0. shown, CAM5 suffers from the ...negative biases of LCA, FLUT, and  $T_{2m}$  during December... January... and February (DJF) (Fig. 9, left panel). In the Arctic during winter, less...he lower LCA in CAM5 reduces FLUT over the land and the...sea-ice region in the lower troposphere the temperature in the cloudy layer is higher than that at the surface (i.e., temperature inversion). Less...he lower LCA also reduces the downward LW radiation at the surface (FLDS), which leads to colder near-surface air than in the reanalysis, resulting in enhancement of...and thus enhances temperature inversion. Compared with CAM5, SAM0 simulates more...reater LCA, FLUT, and  $T_{2m}$  over the whole...ntire Arctic (Fig. 9, center panel), such that their negative biases in CAM5 are alleviated in...y SAM0 (Fig. 9, right panel). Over the ocean where temperature inversion does not exist, more ... [1]

**Deleted:** summertime...ut also the summer biases of TCA, shortwave...W cloud radiative forcing at the TOA (SWCF), and  $T_{2m}$  are also reduced from CAM5 to SAM0 (Fig. 10). In most Arctic areas except for some portions of the northern continents, CAM5 has the...ielded negative biases of ...CA bias during June... July... and August (JJA) (Fig. 10a). SAM0 simulates more...imulated a greater TCA than CAM5 (Fig. 10b), such that most of the negative TCA biases in CAM5 over the Arctic sea ice and open ocean areas disappear (Fig. 10c). The increase of TCA in SAM0 causes the SWCF to decrease (Fig. 10e), which also reduces positive SWCF bias in the vicinity of the Arctic pole (Fig. 10f). In the Arctic during summertime...ummer, cloudiness has the opposite effect on SWCF and LWCF (Supplementary...upplement S7); thus, we need...t is necessary to examine the two radiations...et forcing of SW and LW radiation at the surface to find...etermine the impact of the ...ctic cloud to...louds on the Arctic climate. With more...reater TCA than CAM5, SAM0 simulates more net LW radiation at the surface (FLNS, Fig. 11b). Owing to the high albedo of the underlying sea ice and snow in the vicinity of the Arctic pole, the net SW radiation at the surface (FSNS) does not change much there; however, FSNS decreases substantially in the regions surrounding regions of ...he Arctic pole (Fig. 11a). Overall, the increase of ...n FLNS dominates over the decrease of ...n FSNS in...t the Arctic pole, while the opposite is true in the surrounding regions (Fig...igs. 11b and 11c). The...he net forcing of SW and LW radiation at the surface causes  $T_{2m}$  to increase at the Arctic pole and decrease in the surrounding continental area from CAM5 to SAM0 (Fig. 10h). It is possible that the associated increase of  $T_{2m}$  from CAM5 to SAM0 in the Arctic pole (Fig. 10h) decreases snow depth and surface albedo, while the opposite increases of... but other factors (e.g., less snowfall) may also be responsible for this decrease (Fig. 11d). Less snow depth and ...results in lower surface albedo occur in the surrounding continental area (Fig. 11d and...Fig. 11e). The enhanced SWCF cooling near the Arctic pole in SAM0 (Fig. 10e) is the combined results of the increased TCA and decreased snow depth and ...urface albedo. If the Arctic sea ice fraction is allowed to change in response to the charges of...hanges in the overlying atmospheric conditions (e.g., coupled simulation), SAM0 is likely to simulate less... lower sea ice fraction than CAM5 due to more...he increased TCA and warmer near-surface air temperature, which can be further accelerated by the positive surface albedo feedback (Holland and Bitz, 2003). In fact, Park et al. (2019) found that SAM0 simulates less...ower sea ice fraction than the Community Earth System Model vers[on]

680 4. Summary and Discussion

Many GCMs suffer from cold bias over the Arctic, which has been speculated to be caused by radiation biases associated with cloud fraction and cloud liquid mass underestimation over the Arctic. To address this issue, we compared various aspects of the Arctic clouds and climate in two different AMIP simulations generated by CAM5 and SAM0.

685 Similar to other GCMs and previous studies, CAM5 underestimates the cloud fraction and cloud liquid mass in the Arctic lower troposphere throughout the year. SAM0 alleviates these problems, although biases still persist. Our analysis showed that this improvement in the Arctic cloud simulation with SAM0 is mainly due to the stronger NCD for cloud liquid, which in turn, was due to enhanced poleward transports of heat and moisture by the mean meridional circulation and transient eddies. In SAM0, UNICON strengthens and shifts poleward the zonal mean

690 meridional circulation, polar jet stream, and associated synoptic storm activity on the periphery of the Arctic circle. The proportional relationship between the Arctic cloudiness and meridional transports of heat and moisture exists not only in the CAM5 and SAM0 models, but also in CMIP5 models. Due to the deficient simulations of cloud fraction and cloud liquid mass, CAM5 suffers from negative near-surface air temperature bias throughout the year. With a greater cloud fraction and cloud liquid mass, SAM0 also alleviates the cold temperature biases in 695 the Arctic mainly by enhancing the downward LW radiation at the surface, which is consistent with the hypotheses suggested by previous researchers (Barton et al., 2014; Chan and Comiso, 2013; Klocke et al., 2011; Pithan and Mauritsen, 2014; Walsh and Chapman, 1998). Our study indicates that enhanced poleward heat and moisture transport can improve simulations of Arctic clouds and climate.

Deleted: the

Deleted: underestimated

Deleted: A new unified convection scheme (

Deleted: ) in SAM0

Deleted: in CAM5 and SAM0 also

Deleted: both

Deleted: a set of

Deleted: In association with

Deleted: the

Deleted: bias of

Deleted: more

Deleted: studies

Deleted: the

Deleted: in a model

Deleted: Further study is in progress to investigate this hypothesis using fully coupled model. The authors are also continuously working to further reduce the remaining biases of Arctic clouds and climate by controlling convective activity simulated by UNICON and incorporating an improved ice nucleation scheme as suggested by previous studies.

### Author Contributions

E.-H. Baek performed the overall numerical experiments and analysis. S. Park developed and provided SAM0 and CAM5, and helped analyze the simulation results. B.-M. Kim designed the project and helped analyze the simulation results and the CMIP5 models. All authors contributed to the analyses.

Deleted: ,

Deleted: to

Deleted: to

Deleted: conducting

### Competing interests

The authors declare that they have no conflicts of interest.

Deleted: conflict

### Acknowledgments

This work was supported by the Korea Polar Research Institute projects entitled “Earth System Model-based Korea Polar Prediction System (KPOPS-Earth) Development and Its Application to the High-impact Weather Events originated from the Changing Arctic Ocean and Sea Ice (PE20090).” E.-H. Baek and J.-H. Jeong are supported by the project entitled “Korea-Arctic Ocean Observing System (K-AOOS), KOPRI, 20160245,” funded by the MOF, Korea. S. Park is supported by Seoul National University (SNU). B.-M. Kim is supported by the Korea Meteorological Administration Research and Development Program (grant number KMI2018-03810)

Deleted: project titled ‘Development and Application of the

Deleted: ) for Climate Change and Disastrous

Deleted: (PE19130)’

Deleted: titled ‘

Deleted: 20160245’,

Deleted: the Creative-Pioneering Researchers Program through the ...

Deleted: ) (grant number 3345-20180015

### Data Availability

The data used in this paper are available at [http://gofile.me/6DN3Q/UqIw9dC4i/pub/Paper\\_data/acp2020/](http://gofile.me/6DN3Q/UqIw9dC4i/pub/Paper_data/acp2020/).

## References

- 750 Barton, N. P., Klein, S. A., and Boyle, J. S.: On the ~~contribution of longwave radiation to global climate model~~ ~~biases~~ in Arctic ~~lower tropospheric stability~~, J. Clim., 27, 7250–7269, doi:10.1175/JCLI-D-14-00126.1, 2014.
- Bergeron, T.: Proces ~~verbaux~~ de l'Association de Meteorologie (ed. Duport, P.), International Union of Geodesy and Geophysics, 1935.
- 755 Boe, J., Hall, A., and Qu, X.: Current GCMs' ~~unrealistic negative feedback~~ in the Arctic, J. Clim., 22(17), 4682–4695, doi:10.1175/2009JCLI2885.1, 2009.
- de Boer, G., Chapman, W. L., Kay, J. E., Medeiros, B., Shupe, M. D., Vavrus, S., and Walsh, J. E.: A ~~characterization~~ of the ~~present-day~~ Arctic ~~atmosphere~~ in CCSM4, J. Clim., 25, 2676–2695, doi:10.1175/JCLI-D-11-00228.1, 2012.
- 760 Cesana, G., and Chepfer, H.: How well do climate models simulate cloud vertical structure? A comparison between CALIPSO-GOCCP satellite observations and CMIP5 models, Geophys. Res. Lett., 39(20), 1–6, doi:10.1029/2012GL053153, 2012.
- Cesana, G., Waliser, D. E., Jiang, X., and Li, J.-L. F.: Multi-model evaluation of cloud phase transition using satellite and reanalysis data, J. Geophys. Res. Atmos., (JUNE), n/a-n/a, doi:10.1002/2014JD022932, 2015.
- 765 Chan, M. A., and Comiso, J. C.: Arctic cloud characteristics as derived from MODIS, CALIPSO, and ~~CloudSat~~, J. Clim., 26(10), 3285–3306, doi:10.1175/JCLI-D-12-00204.1, 2013.
- Chapman, W. I., and Walsh, J. E.: Simulations of Arctic temperature and pressure by global coupled models, J. Clim., 20(4), 609–632, doi:10.1175/JCLI4026.1, 2007.
- 770 Chepfer, H., Bony, S., Winker, D., Cesana, G., Dufresne, J. L., Minnis, P., Stubenrauch, C. J., and Zeng, S.: The GCM-oriented CALIPSO cloud product (CALIPSO-GOCCP), J. Geophys. Res. Atmos., 115(5), 1–13, doi:10.1029/2009JD012251, 2010.
- Dee, D. P., Uppala, S. M., Simmons, A. J., Berrisford, P., Poli, P., Kobayashi, S., Andrae, U., Balmaseda, M. A., Balsamo, G., Bauer, P., Bechtold, P., Beljaars, A. C. M., van de Berg, L., Bidlot, J., Bormann, N., Delsol, C., Dragani, R., Fuentes, M., Geer, A. J., Haimberger, L., Healy, S. B., Hersbach, H., ~~Hólm~~, E. V., Isaksen, L., ~~Kållberg~~, P., ~~Köhler~~, M., Matricardi, M., McNally, A. P., Monge-Sanz, B. M., Morcrette, J. J., Park, B. K., Peubey, C., de Rosnay, P., Tavolato, C., ~~Thépaut~~, J. N., and Vitart, F.: The ERA-Interim reanalysis: Configuration and performance of the data assimilation system, Q. J. R. Meteorol. Soc., 137(656), 553–597, doi:10.1002/qj.828, 2011.
- 775 Deser, C., Walsh, J. F., and Timlin, M. S.: Arctic ~~sea ice variability~~ in the ~~context~~ of ~~recent atmospheric~~ Circulation Trends, J. Clim., 13, 617–633, 2000.
- 780 English, J. M., Kay, J. E., Gettelman, A., Liu, X., Wang, Y., Zhang, Y., and Chepfer, H.: Contributions of clouds, surface albedos, and mixed-phase ice nucleation schemes to Arctic radiation biases in CAM5, J. Clim., 27(13), 5174–5197, doi:10.1175/JCLI-D-13-00608.1, 2014.
- English, J. M., Gettelman, A., and Henderson, G. R.: Arctic radiative fluxes: Present-day biases and future projections in CMIP5 models, J. Clim., 28(15), 6019–6038, doi:10.1175/JCLI-D-14-00801.1, 2015.
- 785 Eyring, V., Bony, S., Meehl, G. A., Senior, C. A., Stevens, B., Stouffer, R. J., and Taylor, K. E.: Overview of the Coupled Model Intercomparison Project Phase 6 (CMIP6) experimental design and organization, Geosci. Model Dev., 9(5), 1937–1958, doi:10.5194/gmd-9-1937-2016, 2016.
- Findeisen, W.: Kolloid-Meteorologische, 2nd ed., Am. Meteorol. Soc., Boston, ~~MA~~, 1938.

Deleted: .

Deleted: Contribution

Deleted: Longwave Radiation

Deleted: Global Climate Model Biases

Deleted: Lower Tropospheric Stability

Deleted: Verbaux

Deleted: .

Deleted: .

Deleted: Unrealistic Negative Feedback

Deleted: .

Deleted: Characterization

Deleted: Present-Day

Deleted: Atmosphere

Deleted: .

Deleted: .

Deleted: .

Deleted: .

Deleted: cloudsat

Deleted: .

Deleted: .

Deleted: H??lm

Deleted: K??llberg

Deleted: K??hler

Deleted: Th??paut

Deleted: .

Deleted: .

Deleted: .

Deleted: Sea Ice Variability

Deleted: Context

Deleted: Recent Atmospheric

Deleted: .

Deleted: .

Deleted: .

Deleted: .

Deleted: .

Deleted: .

Deleted: .

Deleted: Mass.,

	Holland, M. M., and Bitz, C. M.: Polar amplification of climate change in coupled models, <i>Clim. Dyn.</i> , 21(3–4), 221–232, doi:10.1007/s00382-003-0332-6, 2003.	Deleted: .
825	Flournoy, M. D., Feldstein, S. B., Lee, S., and Clothiaux, E. E.: Exploring the <b>tropically excited Arctic warming</b> mechanism with station data: Links between tropical convection and Arctic downward infrared radiation, <i>J. Atmos. Sci.</i> , 73(3), 1143–1158, doi:10.1175/JAS-D-14-0271.1, 2016.	Deleted: . Deleted: Tropically Excited Deleted: Warming
830	Hurrell, J. W., Holland, M. M., Gent, P. R., Ghan, S., Kay, J. E., Kushner, P. J., Lamarque, J. F., Large, W. G., Lawrence, D., Lindsay, K., Lipscomb, W. H., Long, M. C., Mahowald, N., Marsh, D. R., Neale, R. B., Rasch, P., Vavrus, S., Vertenstein, M., Bader, D., Collins, W. D., Hack, J. J., Kiehl, J., and Marshall, S.: The community earth system model: A framework for collaborative research, <i>Bull. Am. Meteorol. Soc.</i> , 94(9), 1339–1360, doi:10.1175/BAMS-D-12-00121.1, 2013.	Deleted: .
835	Jiang, H., Cotton, W. R., Pinto, J. O., Curry, J. A., and Weissbluth, M. J.: Cloud <b>resolving simulations of mixed-phase Arctic stratus observed</b> during BASE: Sensitivity to <b>concentration of ice crystals and large-scale heat and moisture advection</b> , <i>J. Atmos. Sci.</i> , 57(13), 2105–2117, doi:10.1175/1520-0469(2000)057<2105:CRSOMP>2.0.CO;2, 2000.	Deleted: . Deleted: Resolving Simulations Deleted: Mixed-Phase Deleted: Stratus Observed Deleted: Concentration Deleted: Ice Crystals Deleted: Large-Scale Heat Deleted: Moisture Advection
	Johannessen, O. M., Kuzmina, S. I., Bobylev, L. P., Martin, W., Johannessen, O. M., Kuzmina, S. I., and Bobylev, L. P.: Tellus <b>A: Dynamic meteorology and oceanography surface</b> air temperature variability and trends in the <b>Arctic: New</b> amplification assessment and regionalization, 0870(May), doi:10.3402/tellusa.v68.28234, 2016.	Deleted: . Deleted: A Deleted: Meteorology Deleted: Oceanography Surface Deleted: Arctic : new
840	Karlsson, J., and Svensson, G.: Consequences of poor representation of Arctic sea-ice albedo and cloud-radiation interactions in the CMIP5 model ensemble, <i>Geophys. Res. Lett.</i> , 40(16), 4374–4379, doi:10.1002/grl.50768, 2013.	Deleted: .
	Kay, J. E., Hillman, B. R., Klein, S. A., Zhang, Y., Medeiros, B., Pincus, R., Gettelman, A., Eaton, B., Boyle, J., Marchand, R., and Ackerman, T. P.: Exposing global cloud biases in the Community Atmosphere Model (CAM) using satellite observations and their corresponding instrument simulators, <i>J. Clim.</i> , 25(15), 5190–5207, doi:10.1175/JCLI-D-11-00469.1, 2012.	Deleted: .
845	Kay, J. E., Bourdages, L., Miller, N. B., Morrison, A., Yettella, V., Chepfer, H., and Eaton, B.: Evaluating and improving cloud phase in the Community Atmosphere Model version 5 using spaceborne lidar observations, <i>J. Geophys. Res. Atmos.</i> , 121(8), 4162–4176, doi:10.1002/2015JD024699, 2016.	Deleted: . Deleted: Sensing Deleted: Liquid Water Deleted: Ice Cloud Optical Thickness Deleted: Effective Radius Deleted: Arctic Deleted: Airborne Multispectral Deleted: Data
850	King, M. D., Platnick, S., Yang, P., Arnold, G. T., Gray, M. A., Riedi, J. C., Ackerman, S. A., and Liou, K.-N.: Remote <b>sensing of liquid water and ice cloud optical thickness and effective radius in the Arctic: Application of airborne multispectral MAS data</b> , <i>J. Atmos. Ocean. Technol.</i> , 21, 857–875, 2004.	Deleted: . Deleted: Effect Deleted: Dynamics Deleted: Mixed-Phase Clouds Deleted: Considerations
855	Klocke, D., Pincus, R., and Quaas, J.: On constraining estimates of climate sensitivity with present-day observations through model weighting, <i>J. Clim.</i> , 24(23), 6092–6099, doi:10.1175/2011JCLI4193.1, 2011.	Deleted: .
	Korolev, A., and Field, P. R.: The <b>effect of dynamics on mixed-phase clouds: Theoretical considerations</b> , <i>J. Atmos. Sci.</i> , 65(1), 66–86, doi:10.1175/2007JAS2355.1, 2008.	Deleted: .
	Kug, J.-S., Jeong, J.-H., Jang, Y.-S., Kim, B.-M., Folland, C. K., Min, S.-K., and Son, S.-W.: Two distinct influences of Arctic warming on cold winters over North America and East Asia, <i>Nat. Geosci.</i> , 8(10), 759–762, doi:10.1038/ngeo2517, 2015.	Deleted: .
860	Lee, S., and Yoo, C.: On the causal relationship between poleward heat flux and the equator-to-pole temperature gradient: A cautionary tale, <i>J. Clim.</i> , 27(17), 6519–6525, doi:10.1175/JCLI-D-14-00236.1, 2014.	Deleted: .

900	Li, J. and Wang, J. X. L.: A modified zonal index and its physical sense, <i>Geophys. Res. Lett.</i> , 30(12), 1–4, doi:10.1029/2003GL017441, 2003.	Deleted: .
905	Liu, X., Xie, S., Boyle, J., Klein, S. A., Shi, X., Wang, Z., Lin, W., Ghan, S. J., Earle, M., Liu, P. S. K. and Zelenyuk, A.: Testing cloud microphysics parameterizations in NCAR CAM5 with ISDAC and M-PACE observations, <i>J. Geophys. Res. Atmos.</i> , 116(24), 1–18, doi:10.1029/2011JD015889, 2011.	Deleted: .
910	Loeb, N. G., Wielicki, B. A., Doelling, D. R., Smith, G. L., Keyes, D. F., Kato, S., Manalo-Smith, N. and Wong, T.: Toward optimal closure of the <u>earth's</u> top-of-atmosphere radiation budget, <i>J. Clim.</i> , 22(3), 748–766, doi:10.1175/2008JCLI2637.1, 2009.	Deleted: . Deleted: Earth's
915	Lu, J. and Cai, M.: Seasonality of polar surface warming amplification in climate simulations, <i>Geophys. Res. Lett.</i> , 36(August), 1–6, doi:10.1029/2009GL040133, 2009.	Deleted: .
920	Madden, R. A. and Julian, P. R.: Detection of a 40–50 <u>day oscillation</u> in the <u>zonal wind</u> in the <u>tropical Pacific</u> , <i>J. Atmos. Sci.</i> , 28(5), 702–708, doi:10.1175/1520-0469(1971)028<0702:DOADOI>2.0.CO;2, 1971.	Deleted: . Deleted: Day Oscillation Deleted: Zonal Wind Deleted: Tropical Deleted: .
925	Morrison, H., Pinto, J. O., Curry, J. A. and McFarquhar, G. M.: Sensitivity of modeled arctic mixed-phase stratocumulus to cloud condensation and ice nuclei over regionally varying surface conditions, <i>J. Geophys. Res. Atmos.</i> , 113(5), 1–16, doi:10.1029/2007JD008729, 2008.	Deleted: .
930	Morrison, H., de Boer, G., Feingold, G., Harrington, J., Shupe, M. D. and Sulia, K.: Resilience of persistent Arctic mixed-phase clouds, <i>Nat. Geosci.</i> , 5(1), 11–17, doi:10.1038/ngeo1332, 2011.	Deleted: .
935	Neale, R. B., Gettelman, A., Park, S., Chen, C., Lauritzen, P. H., Williamson, D. L., Conley, A. J., Kinnison, D., Marsh, D., Smith, A. K., Vitt, F., Garcia, R., Lamarque, J., Mills, M., Tilmes, S., Morrison, H., Cameron-smith, P., Collins, W. D., Iacono, M. J., Easter, R. C., Liu, X., Ghan, S. J., Rasch, P. J. and Taylor, M. A.: Description of the NCAR Community Atmosphere Model (CAM 5.0). NCAR Technical Notes., Tech. Note NCAR/TN-464+STR, 214, doi:10.5065/D6N877R0., 2012.	Deleted: . Deleted: a:
940	Park, S.: A Unified Convection Scheme, UNICON. Part I. Formulation, <i>J. Atmos. Sci.</i> , (Lcl), 140808112307001, doi:10.1175/JAS-D-13-0234.1, 2014a.	
945	Park, S.: A Unified Convection Scheme, UNICON. Part II. Simulation, <i>J. Atmos. Sci.</i> , (Lcl), 140808112307001, doi:10.1175/JAS-D-13-0234.1, 2014b.	
950	Park, S. and Bretherton, C. S.: The University of Washington shallow convection and moist turbulence schemes and their impact on climate simulations with the community atmosphere model, <i>J. Clim.</i> , 22(12), 3449–3469, doi:10.1175/2008JCLI2557.1, 2009.	Deleted: .
955	Park, S., Bretherton, C. S. and Rasch, P. J.: Integrating <u>cloud processes</u> in the Community Atmosphere Model, Version 5, <i>J. Clim.</i> , 27(18), 6821–6856, doi:10.1175/JCLI-D-14-00087.1, 2014.	Deleted: . Deleted: Cloud Processes
960	Park, S., Baek, E.-H., Kim, B.-M. and Kim, S.-J.: Impact of detrained cumulus on climate simulated by the Community Atmosphere Model Version 5 with a unified convection scheme, <i>J. Adv. Model. Earth Syst.</i> , 6, 513–526, doi:10.1002/2016MS000877, 2017.	Deleted: .
965	Park, S., Shin, J., Kim, S., Oh, E., and Kim, Y.: Global climate simulated by the Seoul National University Atmosphere Model Version 0 with a Unified Convection Scheme (SAM0-UNICON), <i>J. Clim.</i> , Accepted. 2019.	Deleted: .
970	Pithan, F. and Mauritsen, T.: Arctic amplification dominated by temperature feedbacks in contemporary climate models, <i>Nat. Geosci.</i> , 7(February), 2–5, doi:10.1038/NGEO2071, 2014.	Deleted: .
975	Pithan, F., Medeiros, B. and Mauritsen, T.: Mixed-phase clouds cause climate model biases in Arctic wintertime temperature inversions, <i>Clim. Dyn.</i> , 43(1–2), 289–303, doi:10.1007/s00382-013-1964-9, 2014.	Deleted: .

	Prenni, A. J., DeMott, P. J., Kreidenweis, S. M., Harrington, J. Y., Avramov, A., Verlinde, J., Tjernström, M., Long, C. N., and Olsson, P. Q.: Can ice-nucleating aerosols affect Arctic seasonal climate?, Bull. Am. Meteorol. Soc., 88(4), 541–550, doi:10.1175/BAMS-88-4-541, 2007.	Deleted: . Deleted: Ice-Nucleating Aerosols Affect Deleted: Seasonal Climate
960	Screen, J. A., and Simmonds, I.: The central role of diminishing sea ice in recent Arctic temperature amplification, Nature, 464(7293), 1334–1337, doi:10.1038/nature09051, 2010.	Deleted: .
	Screen, J. A., and Simmonds, I.: Exploring links between Arctic amplification and mid-latitude weather, Geophys. Res. Lett., 40(5), 959–964, doi:10.1002/grl.50174, 2013.	Deleted: . Deleted: .
965	Sedlar, J., and Tjernström, M.: Stratiform cloud—inversion characterization during the Arctic melt season, Bound.-Layer Meteorol., 132(3), 455–474, doi:10.1007/s10546-009-9407-1, 2009.	Deleted: . Deleted: Cloud—Inversion Characterization During
	Serreze, M. C., and Barry, R. G.: Processes and impacts of Arctic amplification: A research synthesis, Glob. Planet. Change, 77(1–2), 85–96, doi:10.1016/j.gloplacha.2011.03.004, 2011.	Deleted: Melt Season, Boundary- Deleted: .
	Shupe, M. D., and Intrieri, J. M.: Cloud radiative forcing of the Arctic surface: The influence of cloud properties, surface albedo, and solar zenith angle, J. Clim., 17(3), 616–628, doi:10.1175/1520-0442(2004)017<0616:CRFOTA>2.0.CO;2, 2004.	Deleted: ampli fi cation Deleted: .
970	Shupe, M. D., Kollias, P., Persson, P. O. G., and McFarquhar, G. M.: Vertical motions in Arctic mixed-phase stratiform clouds, J. Atmos. Sci., 65(4), 1304–1322, doi:10.1175/2007JAS2479.1, 2008.	Deleted: . Deleted: Motions
	Shupe, M. D., Walden, V. P., Eloranta, E., Uttal, T., Campbell, J. R., Starkweather, S. M., and Shiobara, M.: Clouds at Arctic atmospheric observatories. Part I: Occurrence and macrophysical properties, J. Appl. Meteorol. Climatol., 50(3), 626–644, doi:10.1175/2010JAMC2467.1, 2011.	Deleted: Mixed-Phase Stratiform Clouds Deleted: .
975	Solomon, A., Shupe, M. D., Persson, P. O. G., and Morrison, H.: Moisture and dynamical interactions maintaining decoupled Arctic mixed-phase stratocumulus in the presence of a humidity inversion, Atmos. Chem. Phys., 11(19), 10127–10148, doi:10.5194/acp-11-10127-2011, 2011.	Deleted: .
	Taylor, K. E., Stouffer, R. J., and Meehl, G. A.: An overview of CMIP5 and the experiment design, Bull. Am. Meteorol. Soc., 93(4), 485–498, doi:10.1175/BAMS-D-11-00094.1, 2012.	Deleted: .
980	Walsh, J. E., and Chapman, W. L.: Arctic cloud-radiation-temperature associations in observational data and atmospheric reanalyses, J. Clim., 11(11), 3030–3045, doi:10.1175/1520-0442(1998)011<3030:ACRTAI>2.0.CO;2, 1998.	Deleted: .
	Wegener, A.: Thermodynamik der Atmosphäre, Barth., edited by J. A. Barth, Leipzig, Germany, 1911.	Deleted: .
985	Wielicki, B. A., Barkstrom, B. R., Harrison, E. F., Lee, R. B., Smith, G. L., and Cooper, J. E.: Clouds and the Earth's Radiant Energy System (CERES): An Earth observing system experiment, Bull. Am. Meteorol. Soc., 77(5), 853–868, doi:10.1175/1520-0477(1996)077<0853:CATERE>2.0.CO;2, 1996.	Deleted: Observing System Experiment Deleted: .
	Wu, Y., and Smith, K. L.: Response of Northern hemisphere midlatitude circulation to Arctic amplification in a simple atmospheric general circulation model, J. Clim., 29(6), 2041–2058, doi:10.1175/JCLI-D-15-0602.1, 2016.	Deleted: Hemisphere Midlatitude Circulation Deleted: Amplification Deleted: Simple Atmospheric General Circulation Model
990	Xie, S., Liu, X., Zhao, C., and Zhang, Y.: Sensitivity of CAM5 simulated Arctic clouds and radiation to ice nucleation parameterization, J. Clim., 26, 5981–5999, doi:10.1175/JCLI-D-12-00517.1, 2013.	Deleted: . Deleted: Simulated Deleted: Clouds Deleted: Radiation
	Zhang, G. J., and McFarlane, N. A.: Role of convective scale momentum transport in climate simulation, J. Geophys. Res. Atmos., 100(D1), 1417–1426, doi:10.1029/94JD02519, 1995.	Deleted: Ice Nucleation Parameterization, J.
995	Xie, S., McCoy, R. B., Klein, S. A., Cederwall, R. T., Wiscombe, W. J., Clothiaux, E. E., Gaustad, K. L., Golaz, J. C., Hall, S. D., Jensen, M. P., Johnson, K. L., Lin, Y., Long, C. N., Mather, J. H., McCord, R. A., McFarlane,	Deleted: . Deleted: a Deleted: a



S. ~~A.~~, Palanisamy, G., Shi, Y. ~~a~~, and Turner, D. D.: ARM climate modeling best estimate data: A new data product for climate studies, Bull. Am. Meteorol. Soc., 91(1), 13–20, doi:10.1175/2009BAMS2891.1, 2010.

Deleted: a

Deleted: .

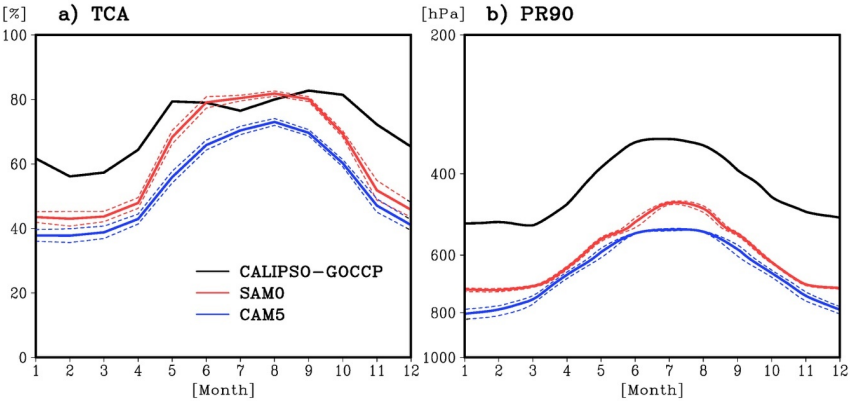


Figure 1: Annual cycles of the (a) total cloud fraction (TCA) and (b) height at which the ratio of ice condensate mass to total condensate mass is 90 % (phase ratio, PR90) averaged over the Arctic area, north of 65° N from CALIPSO-GOCCP observations averaged from June 2006 to November 2010 (black line), SAM0 (red line), and CAM5 (blue line). The dashed lines denote the standard deviations of the variables. The CALIPSO-GOCCP observations were averaged from June 2006 to November 2010, and the model results are the means of AMIP simulation results for 36 years from January 1979 to February 2015.

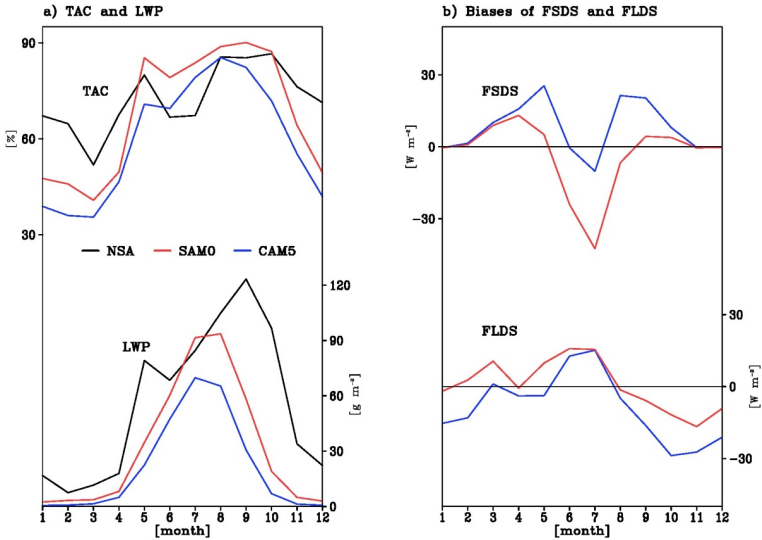
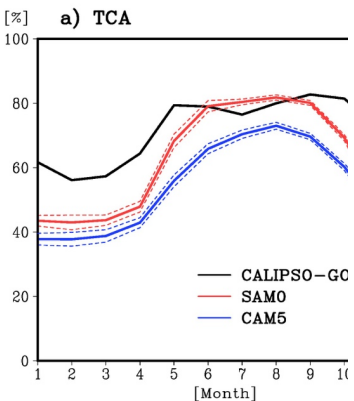


Figure 2: Annual cycles of total cloud fraction (TAC, upper in (a)) and liquid water path (LWP, bottom in (a)) from the climatology of ground-based cloud and radiation measurements at the North Slope of Alaska (NSA) Barrow site (black line), SAM0 (red line), and CAM5 (blue line). Biases of surface downward SW flux (FSDS, upper in (b)) and surface downward longwave flux (FLDS, bottom in (b)) of SAM0 (red line) and CAM5 (blue line) against the NSA Barrow site (black line).



Deleted:

Deleted: the

Deleted: where

Deleted: Dashed

Deleted: deviation

Deleted: each variable

Formatted: Font: Not Bold, Not Italic

Deleted: ),

Deleted: shortwave

Deleted: ),

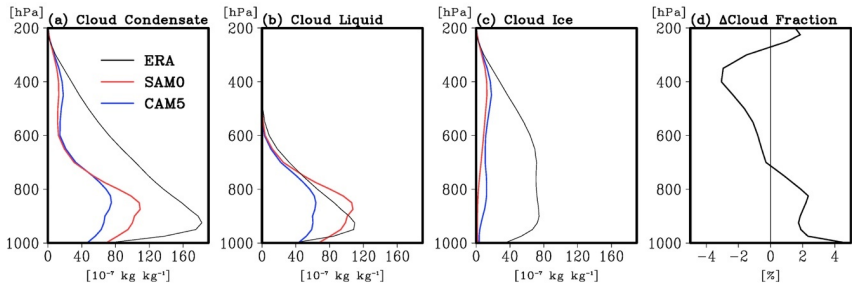
Deleted: from

1060

climatology of ground-based cloud and radiation measurements at NSA Barrow site. The NSA Barrow site observations were averaged from 1998 to 2010, and the model results are the means of AMIP simulation results for 36 years from January 1979 to February 2015.

Deleted: North Slope of Alaska (

Deleted: )



1065

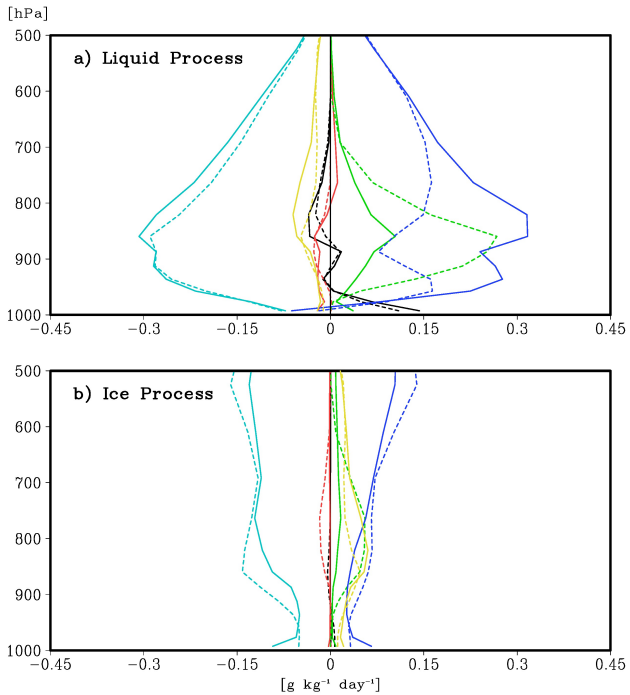
Figure 3: Annual-mean vertical profiles of grid-mean (a) cloud condensate mass (cloud liquid + cloud ice), (b) cloud liquid mass, and (c) cloud ice mass averaged over the Arctic from ERA-Interim reanalysis (ERA, black lines), SAM0 (red lines) and CAM5 (blue lines), and (d) the difference in cloud fraction between SAM0 and CAM5. ERA-Interim reanalysis was averaged from January 1979 to February 2015, and the model results are the means of AMIP simulation results for 36 years from January 1979 to February 2015.

Deleted:

Deleted: area

Deleted: interim

Deleted: of

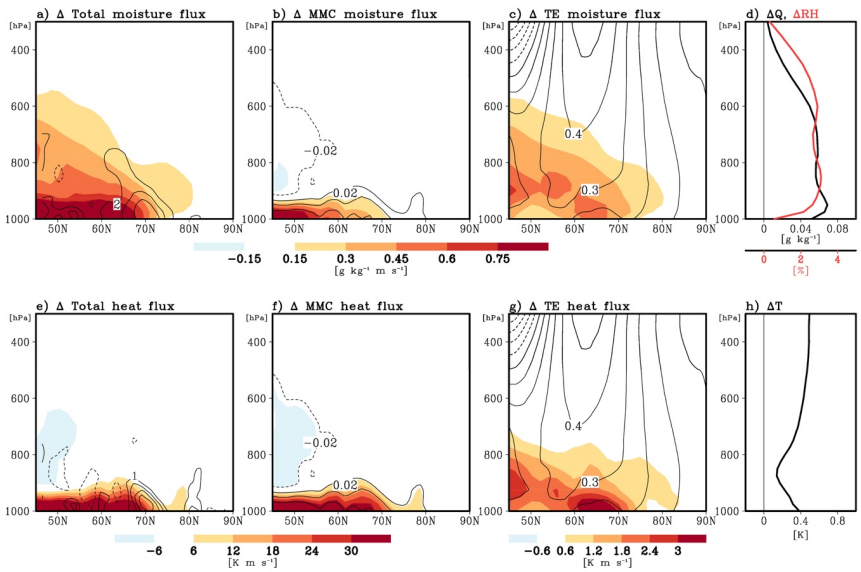


1070

1080

Figure 4: Annual-mean vertical profiles of the grid-mean tendencies of the (a) cloud liquid mass and (b) cloud ice mass induced by various moist physics processes from SAM0 (solid lines) and CAM5 (dotted lines). The processes shown are subgrid vertical transport by local symmetric turbulent eddies (PBL, black), subgrid vertical transport by nonlocal asymmetric turbulent eddies (CON, red), convective detrainment (DET, green), net condensation of water vapor into cloud liquid and net deposition of water vapor into cloud liquid and ice (NCD, blue), precipitation-sedimentation fallout (PRS, cyan), and WBF conversion from cloud liquid mass to cloud ice mass (WBF, yellow).

Deleted: color



1085

Figure 5: Differences in zonal-mean meridional fluxes of (a, b, and c) moisture and (e, f, and g) heat due to (a and e) total processes (i.e., the transported sum by mean meridional circulation, stationary eddies, and transient eddies), (b and f) mean meridional circulation (MMC), and (c and g) transient eddies (TE) between SAM0 and CAM5. Differences in the annual-mean vertical profiles (d) water vapor (Q, black) and relative humidity (RH, red), and (h) air temperature (T) averaged over the Arctic between SAM0 and CAM5. The black lines in (a) and (e) denote the differences in zonal-mean convergence of total moisture flux in  $10^{-7} \text{ g kg}^{-1} \text{ m s}^{-1}$  and total heat flux in  $10^{-5} \text{ K s}^{-1}$ . The black lines in (b) and (f) denote the differences in zonal mean meridional wind in  $\text{m s}^{-1}$ . The black lines in (c) and (g) denote the differences in zonal-mean zonal wind in  $\text{m s}^{-1}$  between SAM0 and CAM5, respectively. Most shaded areas exceed 95 % significance level from the Student t-test.

Deleted: of

Deleted: by

Deleted: of

Deleted: area

Deleted: of

Deleted: of

Deleted: of

1090

1105

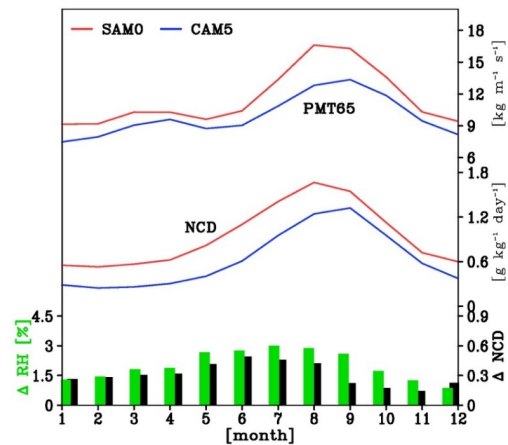
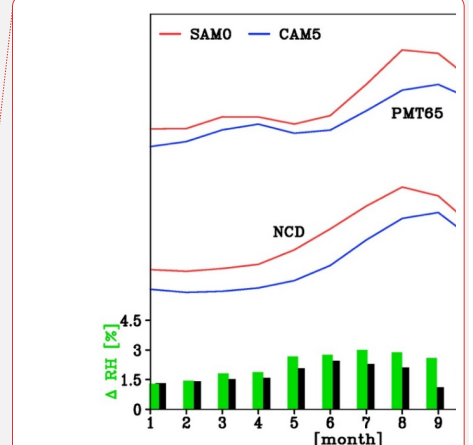


Figure 6: Annual cycles of vertically integrated zonal-mean poleward moisture transport in  $\text{g kg}^{-1} \text{m s}^{-1}$  at  $65^\circ \text{N}$  (PMT65) and net condensation rate of water vapor into cloud liquid (NCD) in  $\text{g kg}^{-1} \text{day}^{-1}$  averaged over the Arctic from SAM0 (red line) and CAM5 (blue line).



Deleted:

Deleted: -

Deleted: area

1110

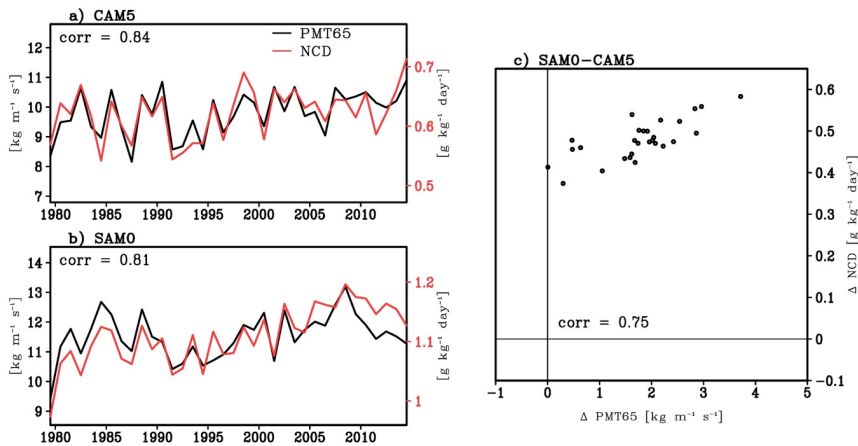


Figure 7: Interannual time series of the vertically integrated annual-mean poleward moisture flux at  $65^\circ \text{N}$  (PMT65, black line) and net condensation rate of water vapor into cloud liquid (NCD, red line) averaged over the Arctic from (a) CAM5 and (b) SAM0, and (c) scatter plot of the differences in annual-mean PMT65 and NCD between SAM0 and CAM5.

Deleted: -

Deleted: area

Deleted: the

Deleted: of

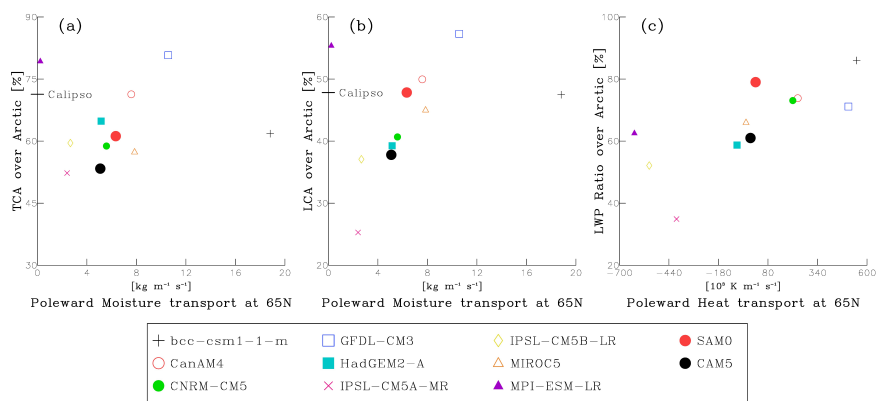


Figure 8: Scatter plots of the annual mean poleward fluxes of moisture and heat integrated over the vertical layers (1000–7000 hPa) at 65° N, cloud fractions, and LWP ratio averaged over the Arctic, obtained from various AMIP simulations of CMIP5 models, CAM5, and SAM0. The black lines in (a) and (b) denote the observed TCA and LCA, respectively, obtained from CALIPSO-GOCCP data.

Deleted: area

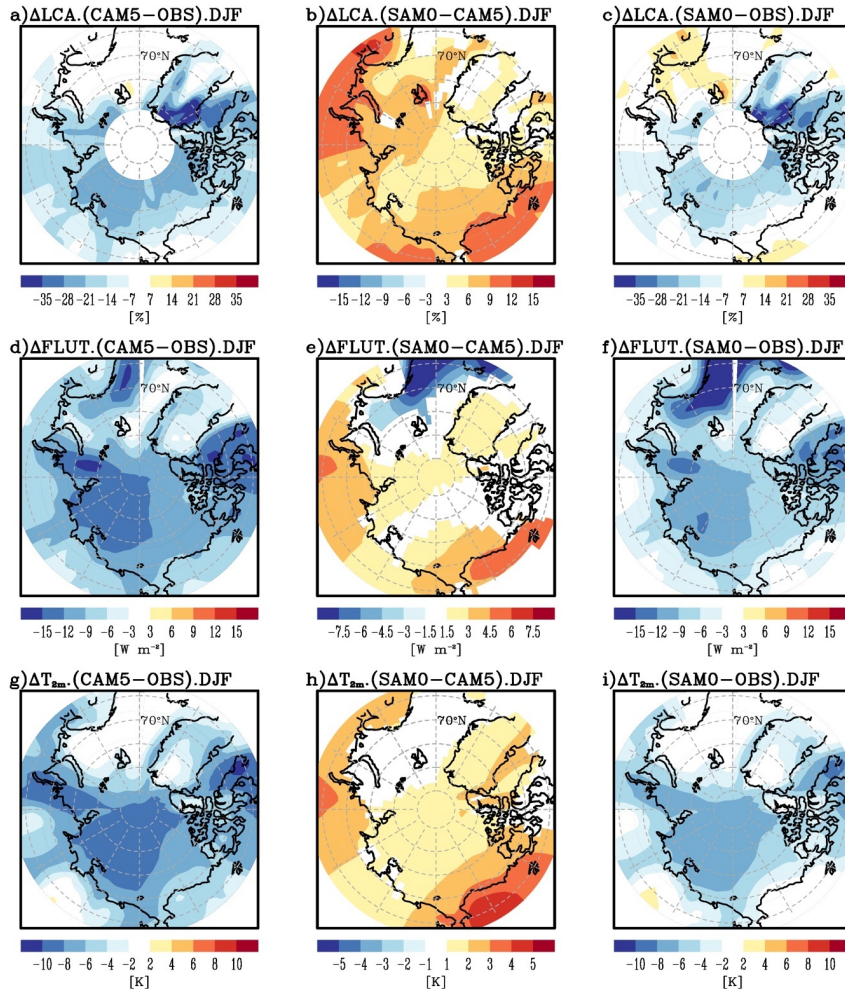


Figure 9: Biases of (upper) low cloud fraction (LCA) against the CALIPSO-GOCCP observation, (middle) upward longwave (LW) radiative flux at TOA (FLUT) against the CERES-EBAF observation, and (lower) near-surface air temperature at a 2 m height ( $T_{2m}$ ) against the ERA-Interim reanalysis during DJF obtained from (left) CAM5 and (right) SAM0, and (center) the differences in each variable between SAM0 and CAM5. The CERES-EBAF observations were averaged from 2000 to 2013, ERA-Interim reanalysis was averaged from January 1979 to February 2015, and the model results are the means of AMIP simulation results for 36 years from January 1979 to February 2015. Shaded areas in (b), (e), and (h) exceed 95 % significance level from the Student t-test.

Deleted:

Deleted: interim

Deleted: of



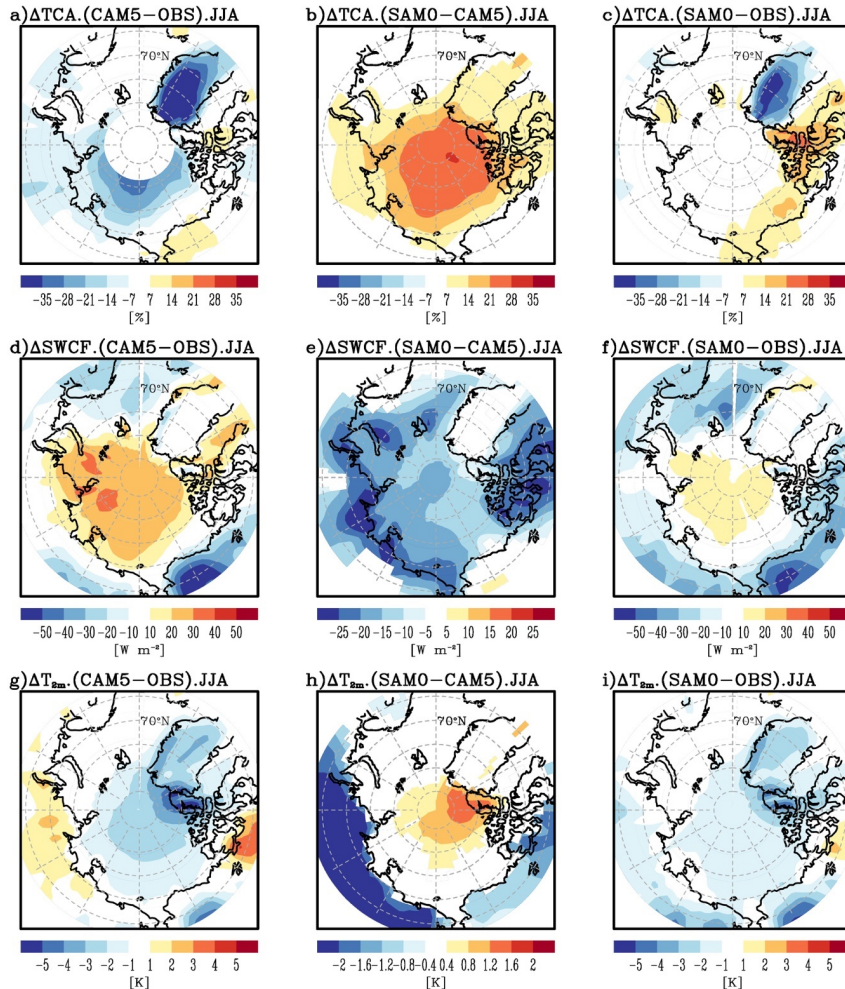
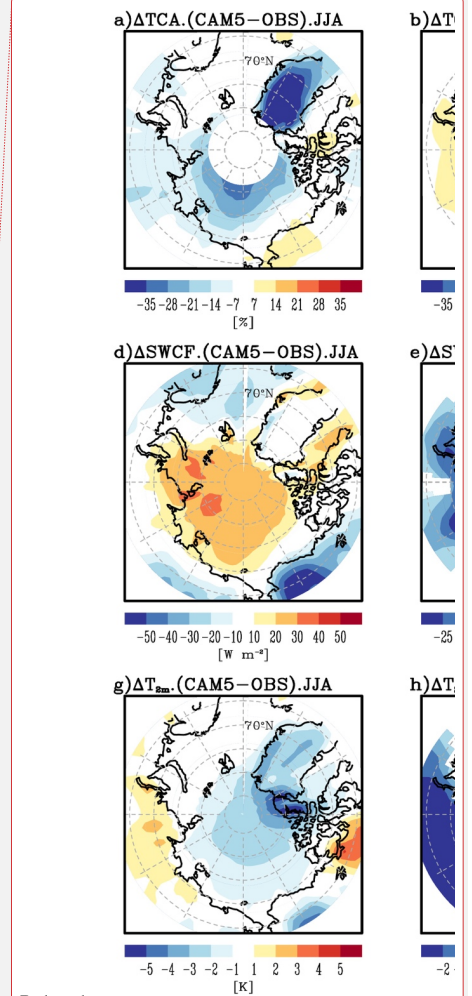


Figure 10: Identical with Fig. 8, except for total cloud fraction (TCA) in the upper panel, the **SW** cloud radiative forcing at TOA (SWCF) in the middle panel, and during JJA.



Deleted:

Deleted: shortwave

Deleted: Shaded areas in (b), (e), and (h) exceed 95 % significance level from the Student t-test.

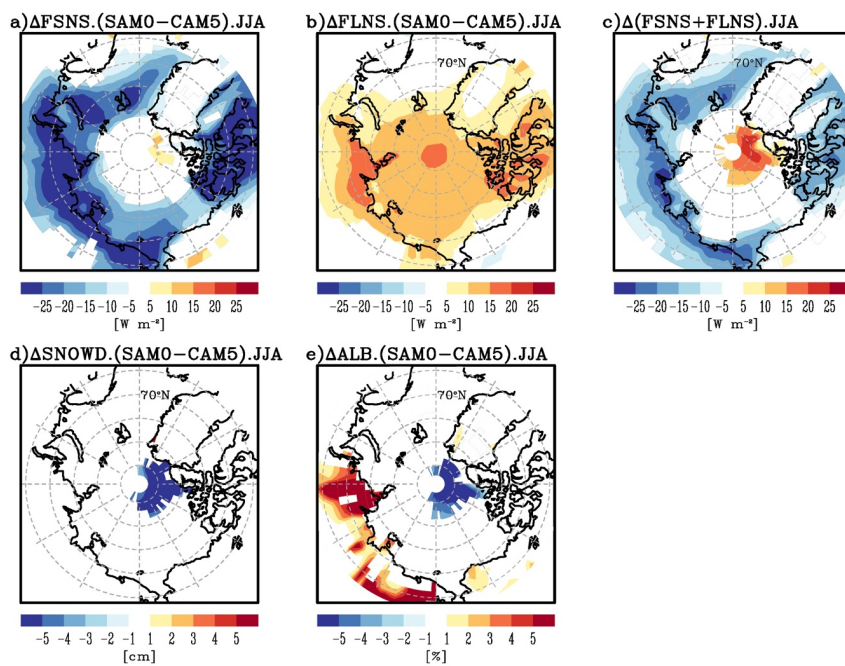
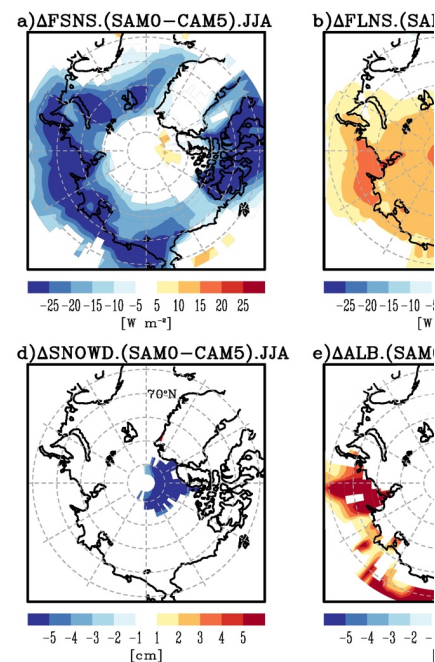


Figure 11: Differences of (a) net SW flux at the surface (FSNS), (b) net LW flux at the surface (FLNS), (c) sum of FSNS and FLNS, (d) snow depth (SNOWD), and (e) surface albedo (ALB) during JJA between SAM0 and CAM5. Shaded areas exceed 95 % significance level from the Student t-test.

Deleted: ¶



Formatted: Caption, Space After: 10 pt

Deleted: ¶

Page 8: [1] Deleted

Author

Page 8: [1] Deleted

Author

Page 8: [1] Deleted

Author

Page 8: [1] Deleted

Author

Page 8: [1] Deleted

Author

Page 8: [1] Deleted

Author

Page 8: [1] Deleted

Author

Page 8: [1] Deleted

Author

Page 8: [1] Deleted

Author

Page 8: [1] Deleted

Author

Page 8: [1] Deleted

Author

Page 8: [1] Deleted

Author

Page 8: [1] Deleted

Author

Page 8: [1] Deleted

Author

Page 8: [2] Deleted

Author

Page 8: [2] Deleted

Author

Page 8: [2] Deleted

Author

Page 8: [2] Deleted

Author

Page 8: [2] Deleted

Author

Page 8: [2] Deleted

Author

Page 8: [2] Deleted

Author

Page 8: [2] Deleted

Author

Page 8: [2] Deleted

Author

Page 8: [2] Deleted

Author

Page 8: [2] Deleted

Author

Page 8: [2] Deleted

Author

Page 8: [2] Deleted

Author

Page 8: [2] Deleted

Author

Page 8: [2] Deleted

Author

Page 8: [2] Deleted

Author

Page 8: [2] Deleted

Author

Page 8: [2] Deleted

Author

Page 8: [2] Deleted

Author

Page 8: [2] Deleted

Author

Page 8: [2] Deleted

Author

Page 8: [2] Deleted

Author

Page 8: [2] Deleted

Author

Page 8: [2] Deleted

Author

Page 8: [2] Deleted

Author

Page 8: [2] Deleted

Author

Page 8: [2] Deleted

Author

Page 8: [2] Deleted

Author

Page 8: [2] Deleted

Author

Page 8: [2] Deleted

Author

Page 8: [2] Deleted

Author

Page 8: [2] Deleted

Author

Page 8: [2] Deleted

Author